Finite element modelling and load share analysis for involute worm gears with localized tooth contact

F Yang, D Su* and **C R Gentle**
Department of Mechanical and Manufacturing Engineering, The Nottingham Trent University, Nottingham, UK

Abstract: A new approach has been developed by the authors to estimate the load share of worm gear drives, and to calculate the instantaneous tooth meshing stiffness and loaded transmission errors. In the approach, the finite element (FE) modelling is based on the modified tooth geometry, which ensures that the worm gear teeth are in localized contact. The geometric modelling method for involute worm gears allows the tooth elastic deformation and tooth root stresses of worm gear drives under different load conditions to be investigated. On the basis of finite element analysis, the instantaneous meshing stiffness and loaded transmission errors are obtained and the load share is predicted. In comparison with existing methods, this approach applies loaded tooth contact analysis and provides more accurate load capacity rating of worm gear drives.

Keywords: worm gears, load share analysis, localized tooth contact, transmission errors

NOTATION

a, b	major and minor semi-axes of contact area respectively
A, B, C	auxiliary parameters used for contact deflection calculation
A_h	centre distance of hob mounting
A_0	centre distance of the worm gear drive
c_δ, c_b	coefficients for contact deflection
$\boldsymbol{d}$	vector for torque distribution
E	Young's modulus
F_δ	instantaneous load at the contact point
$k_\mathrm{I}^{(i)}, k_\mathrm{II}^{(i)}$	principal curvatures of the contact surfaces ($i = 1, 2$)
K_δ	instantaneous meshing stiffness at the contact point
$\mathbf{M}_{21}$	matrix of transmission from Σ_1 to Σ_2
$\boldsymbol{n}'$	normal of the modified worm and wheel
$\boldsymbol{n}_\mathrm{ref}$	normal to tooth surface at the reference point
$\boldsymbol{n}_\mathrm{M}^{(2)}$	normal vector at a meshing point
p	pitch
p_nh	normal pitch of the hob
p_nw	normal pitch of the modified worm
p_0	maximum pressure at the centre of the contact area
P	total load

$P_{x,y}$	contact pressure at a point within the contact area
r_f	radius of the reference circle of the wheel
$\boldsymbol{r}_\mathrm{M}^{(2)}$	hob mounting position vector
$\boldsymbol{r}_1, \boldsymbol{r}_2$	vectors of worm and wheel surfaces respectively
r_{01}	worm pitch radius
R_i	rotation radius of the contact point
$\boldsymbol{T}$	torque vector
TE_i	real transmission error
u	worm cutting tool parameter
U	sum of elastic deformation$= U_1 + U_2$
U_1	deformations of the worm tooth
U_2	deformations of the wheel tooth
$\boldsymbol{v}'^{(12)}$	relative velocity of the modified worm and wheel
$\boldsymbol{v}_\mathrm{ref}$	relative velocity between worm and wheel at a reference point
δ	elastic deflection
δ_1	worm thread lead angle
$\boldsymbol{\delta}$	vector of the elastic deformation
$\boldsymbol{\Delta}$	vectors to describe the total displacement
$\Delta\boldsymbol{\theta}$	rotation increment at a contact point
$\Delta\varphi_i$	theoretical transmission error without consideration of loading
$\zeta^{(12)}$	angle formed by the unit vectors in the principal directions
θ_h	hob mounting angle
λ	compensation angle of the wheel owing to tooth modification
ν	Poisson's ratio

Σ_u coordinate system rigidly connected to the worm cutter

Σ_1 coordinate system rigidly connected to the worm

Σ_2 coordinate system rigidly connected to the wheel

τ displacement caused by the transmission error

ϕ_u worm cutting tool rotation angle with respect to the worm

ϕ_1, ϕ_2 rotation angles of the worm and wheel respectively

Subscripts

u refers to coordinate systems Σ_u
1   refers to coordinate systems Σ_1
2   refers to coordinate systems Σ_2
ref   refers to the reference point

1 INTRODUCTION

Conventional worm gear drives are sensitive to manufacturing and assembly errors owing to the fact that they are designed on the assumption that the conjugated worm gear tooth surfaces are in line contact. In reality, however, line contact is almost impossible to achieve on account of manufacturing and assembly errors and deflection under loading; instead, worse situations such as edge contact occur which severely reduce the loading capacity and, hence, the service life of worm gear drives.

Much research attention has been directed to improving the tooth contact of worm gearing. At an early stage, attempts were made deliberately to introduce manufacturing errors to improve bearing contact [1, 2]. Recently, localized tooth contact has been introduced to provide an ideal bearing contact with low sensitivity to errors. Among existing achievements, there are two main approaches:

(a) tooth geometry modification of worm gear drives to achieve localized contact for which some methods were developed by Vinula et al. [3] and Yoshino and Muta [4];
(b) numerical methods for tooth contact analysis of localized contact for worm gear drives [5, 6].

These developments provide the theoretical basis for a better understanding of localized tooth contact for worm gear drives. However, although the existing methods may achieve localized contact, they cannot ensure that the contact area is placed at an ideal position and so the meshing quality is uncontrollable. In addition, since the localized contact is affected by the load applied and tooth geometry, and existing methods do not provide a proper means to evaluate load share, the contact area can only be roughly estimated.

Stress analysis of gears generally assumes a uniform load distribution along an ideal contact line. Although this is known to be an oversimplification, it is still applied in practice because of the complexity of the tooth geometry and the lack of an effective alternative methodology. Owing to manufacturing errors and various factors such as elastic deformation under load, tooth profile modification, misalignment and wear, the ideal line contact never occurs in practice and the load distribution on the tooth surface is far from uniform. The contact lines degenerate into contact areas whose size and position vary with load. Therefore, the results of analysis using the existing methods are only rough estimates and disagree with the real situation.

The loading capacity and transmission quality of worm gearing depend on the behaviour of the worm gear tooth contact under load. The current existing analysis methods are mainly empirical ones, which are based on simplified test data, and mathematical models that assume ideal tooth loading. Obviously, design based on these methods is unlikely to achieve optimum capacity of the worm gears. Loaded tooth contact analysis (LTCA), which is based on the application of finite element analysis to determine load sharing between the teeth, real contact ratio and stresses, is desired for better worm gear design. With LTCA, the deformation of teeth, stresses in gears and load distribution between teeth can be estimated more accurately. Considerable work has been done for other types of gear drives [7, 8], but LTCA for worm gear drives has not been seen.

A general approach has been developed by the authors for finite element (FE) modelling and load share analysis of involute worm gear with localized tooth contact, which is reported in this paper. The approach is based on the LTCA and provides more accurate rating of loading capacity of worm gear drives than existing methods. In the following sections, the principles of the approach are presented, including the design of worm gear with localized tooth contact, FE modelling and determination of the localized contact area; then the load sharing among the multiple tooth pairs in mesh and the transmission errors are analysed, on the basis of the results obtained using the approach.

2 DESIGN OF WORM GEARS WITH LOCALIZED TOOTH CONTACT

In order to achieve localized tooth contact for involute worm gear drives, the following basic ideas are adopted for modifying the worm gear tooth profiles:

(a) reduce the worm diameter and increase the lead angle of the worm;
(b) make the modified worm have the same normal pitch at the reference point as the original one;

(c) change the hob mounting angle, θ_h, to modify the wheel tooth surface.

For a conventional involute worm, which is equivalent to the hob used to produce the wheel, the tooth surface is given by

$$
\boldsymbol{r}_1 = \boldsymbol{r}_1(u, \phi_u) = \begin{pmatrix} x_1 \\ y_1 \\ z_1 \\ 1 \end{pmatrix}
$$

$$
= \begin{pmatrix} r_{01} \cos \phi_u + u \cos \delta_1 \sin \phi_u \\ r_{01} \sin \phi_u - u \cos \delta_1 \cos \phi_u \\ -u \sin \delta_1 + p \phi_u \\ 1 \end{pmatrix} \quad (1)
$$

The worm wheel tooth surface is the envelope of the family of worm surfaces, and hence

$$
\boldsymbol{r}_2 = \boldsymbol{r}_2(u, \phi_u, \phi_1)
$$

$$
= \mathbf{M}_{21} \cdot \boldsymbol{r}_1(u, \phi_u), \qquad f(u, \phi_u, \phi_1) = 0 \quad (2)
$$

$\mathbf{M}_{21}$

$$
= \begin{bmatrix} \cos \phi_1 \cos \phi_2 & -\sin \phi_1 \cos \phi_2 & -\sin \phi_2 & A_0 \cos \phi_2 \\ -\cos \phi_1 \sin \phi_2 & \sin \phi_1 \sin \phi_2 & -\cos \phi_2 & -A_0 \sin \phi_2 \\ \sin \phi_1 & \cos \phi_1 & 0 & 0 \\ 0 & 0 & 0 & 1 \end{bmatrix}
$$

In equation (2), $f = 0$ is the equation of worm–wheel meshing.

The procedure to determine the modification parameters is briefly described below (for further details, see reference [9]):

Step 1. Determine the reference contact point for design. The reference point is the point on the tooth surface where localized contact occurs with the theoretical transmission ratio during tooth meshing. It is used as a design reference and is chosen by the designer. With equations (1) and (2), the reference point on the wheel tooth surface can be represented by

$$
\boldsymbol{r}_{\text{ref}} = \boldsymbol{r}_2'(r_{\text{f}}, \phi_u, \phi_1) = \mathbf{M}_{21} \cdot \boldsymbol{r}_1(u_{\text{ref}}, \phi_u) \quad (3)
$$

Step 2. Determine the meshing point of the modified tooth surfaces. The modified tooth surface of the wheel is different from the original one. As shown in Fig. 1, to ensure that it is in tangency with the worm at the reference point, it has to be turned into the right position around the wheel axis with an angle λ, in
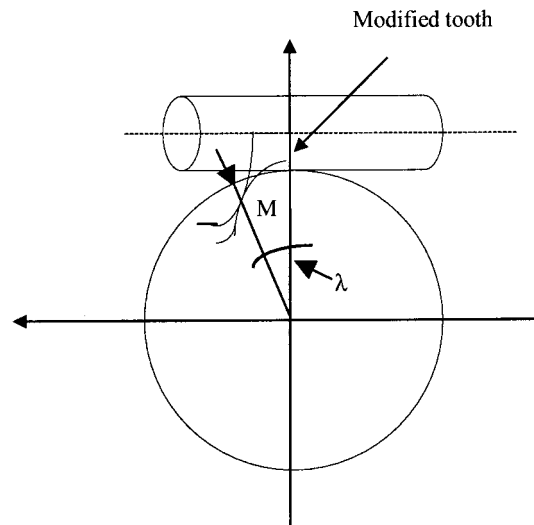

Fig. 1 Meshing position of the modified tooth

order to eliminate the gap between the worm and wheel tooth surfaces; λ is a function of the normal $\boldsymbol{n}_{\text{ref}}$ and relative velocity $\boldsymbol{v}_{\text{ref}}$, i.e.

$$
\lambda = \lambda(\boldsymbol{n}_{\text{ref}}, \boldsymbol{v}_{\text{ref}}) \quad (4)
$$

Step 3. Determine the hob mounting parameters. During modification, a normal hob is used to manufacture the wheel with a specific mounting angle θ_h and centre distance A_h. The hob mounting angle θ_h is given by the designer, while the mounting centre distance of the hob can be obtained as below:

$$
A_h = r_{Mx}^{(2)} - r_{Mz}^{(2)} \frac{n_{Mx}^{(2)}}{n_{Mz}^{(2)}} - p \frac{n_{My}^{(2)}}{n_{Mz}^{(2)}} \quad (5)
$$

where $\boldsymbol{r}_M^{(2)}$ and $\boldsymbol{n}_M^{(2)}$ are the position and normal vectors of the meshing point respectively, which can be calculated by rotating the corresponding vectors of the reference point through an angle λ. Then, the centre distance for hob mounting is determined by equation (5). Thus, the parameters of hob mounting are now determined.

Step 4. Determine the worm modification parameters. After modification, the modified worm gear drives should still satisfy the meshing equation. Thus, by solving the set of equations consisting of the meshing equation and the condition for the modification proposed, as shown below, the design parameters of the modified worm can be obtained, including its diameter, lead angle and the centre distance of the modified worm gear drive:

$$
\boldsymbol{n}' \cdot \boldsymbol{v}'^{(12)} = 0
$$

$$
p_{nh} = p_{nw}
$$

$$
(6)
$$

where n' and $v'^{(12)}$ are the normal and relative velocity of the modified worm gear drive, and p_{nh} and p_{nw} are the normal pitch of the hob and the modified worm respectively.

All the modification design parameters can be determined using the method described above. However, the hob mounting angle and the pitch of the modified worm need to be given by the designer initially, and may be modified later according to the results of tooth contact analysis. Based on the modified design parameters, FE models of worm and wheel can be obtained.

3 FINITE ELEMENT MODELLING FOR INVOLUTE WORM GEARS

The FE modelling of the worm wheel consists of several steps. The first step is to create accurate geometric models for the three-dimensional tooth profile, which is completed using software package Pro/Engineer [10]. The three-dimensional models created in Pro/Engineer are exported as an IGES file that is a standard file format for graphic exchange. Then, the IGES files are imported into the software ANSYS 5.3 [11]. When the IGES file is retrieved in ANSYS, it is usually only a geometric model with the surface information. Within the preprocessor of ANSYS, it is necessary to merge the surfaces to create proper volumes. After that, the proper element type and material property need to be chosen and the mesh of models will be performed.

3.1 Finite element model of wheel

Owing to the complexity of the tooth surface geometry, it is difficult to apply mapped meshing for the wheel model. In order to resolve this problem, it is necessary to divide the body into some individual units of six-sided volumes so that the software can implement the mapped mesh. In this research, the IGES file is imported into ANSYS 5.3 and a part of the wheel body containing six teeth is created using the surface geometry obtained from the IGES file. The whole volume is further divided into 57 subvolumes which are suitable for mapped meshing. The gear wheel body with 57 individual volumes and areas is shown in Fig. 2.

An involute cylindrical gear wheel model with 56 teeth and speed ratio 3/56 reduction is created. The throat radius of the wheel is 37.160 mm and the outside diameter is 500 mm. The gear face width is 78.0 mm. The 20-noded element (solid-95) is used to mesh the model, and the mesh result for the whole model can be seen in Fig. 3.

3.2 Finite element model of worm.

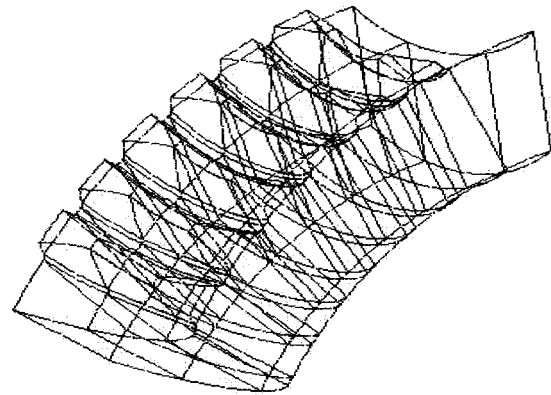To create a whole model of the worm, the authors developed a useful approach for FE modelling of

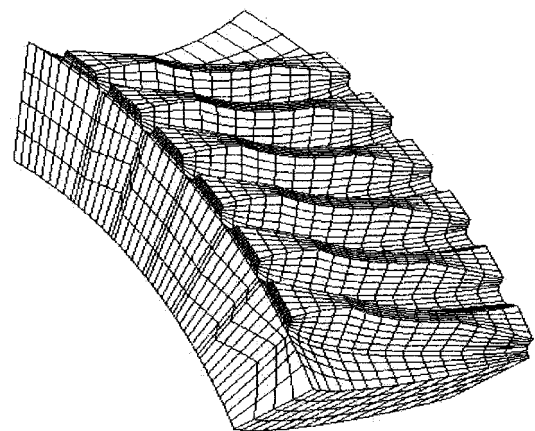**Fig. 2** Individual volumes for mapped mesh

Fig. 3 Finite element mesh of the wheel model

helical geometry. The idea to develop a complete worm FE mesh is based on the fact that mesh extrusion of shell elements can generate three-dimensional elements and this function can produce elements to fit helical shapes such as worm profiles. A function command called VEXT operation in ANSYS 5.3 is applied to perform the mesh extrusion. Because a rotation of the shell elements around an axis is allowed during the VEXT operation, the extrusion process is able to produce a helical shape mesh. The FE model generated using VEXT is shown in Fig 4.

4 DETERMINATION OF THE LOCALIZED TOOTH CONTACT AREA

Theoretically, the tooth pairs of a conventional worm gear drive are in line contact. However, for worm gear drives with localized tooth contact, the worm and gear teeth initially contact at a point. Owing to the tooth elastic deformation under load, the contact zone is
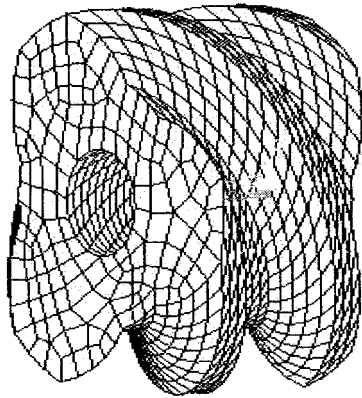
Fig. 4 Finite element mesh of the whole worm model

spread over an elliptical area centred on the theoretical contact point.

4.1 Hertzian assumption

For an elastic and isotropic material, Hertz proposed assumptions for the general contact loading case. He showed that the intensity of pressure between the contacting surfaces could be represented by the semi-ellipsoid construction shown in Fig. 5.

The contact pressure at any point within the contact area is expressed as

$$p_{x,y} = p_0 \sqrt{1 - \frac{x^2}{a^2} - \frac{y^2}{b^2}} \tag{7}$$

where p_0 is the maximum pressure at the centre of the contact area, and a and b are the major and minor semi-axes respectively. The total load is then given by the volume of the semi-ellipsoid:

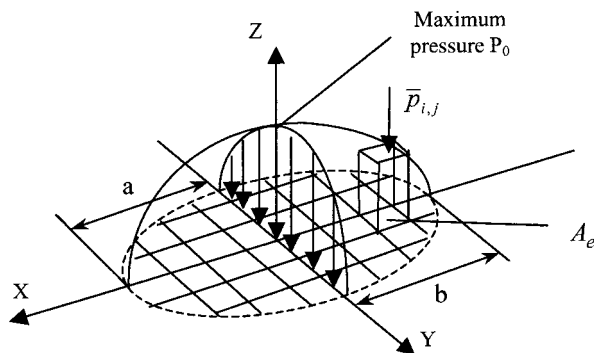$$P = \tfrac{2}{3}\pi a b p_0 \tag{8}$$

Fig. 5 Finite element representation of Hertzian contact pressure

Therefore, the maximum pressure p_0 is given in terms of the applied load as

$$p_0 = \frac{3P}{2\pi ab} \tag{9}$$

4.2 Determination of the contact ellipse

For any given contact load P it is necessary to determine the value of the major and minor axes before the maximum contact stress can be evaluated. The following procedure can be applied to determine the axes of the contact ellipse.

4.2.1 Calculation of the deflection of the contact bodies

The method of deflection evaluation is proposed below and consists of three steps:

(a) computation of the auxiliary parameters,
(b) selection of the deflection coefficients,
(c) determination of the elastic deflection.

Equations of elastic deflection and contact ellipse. From the theory of contact mechanics [12], the expression for the elastic deflection δ is given as

$$\delta = c_\delta \frac{P}{\pi} \left(\frac{A+B}{b/C} \right) \tag{10}$$

$$b = c_b \sqrt[3]{PC} \tag{11}$$

$$a = \sqrt{\left| \frac{\delta}{A} \right|} \tag{12}$$

Actually, the deflection δ expresses the sum of the 'deflections' of the two contact bodies as they approach each other. In equation (10), A, B and C are auxiliary parameters used for calculating the deflection of bodies in point contact, and c_δ and c_b are the coefficients.

Computation of auxiliary parameters. Parameter C is a function of the elastic constants E and ν of the contact bodies and is given as

$$C = \frac{1}{A+B} \left(\frac{1-\nu_1^2}{E_1} + \frac{1-\nu_2^2}{E_2} \right) \tag{13}$$

where A and B are related to the surface curvature of the contact bodies and can be expressed [12] as

$$A = \tfrac{1}{4}(k_{\mathrm{I}}^{(1)} + k_{\mathrm{II}}^{(1)} + k_{\mathrm{I}}^{(2)} + k_{\mathrm{II}}^{(2)})$$

$$- \tfrac{1}{4}\sqrt{\begin{array}{c}[(k_{\mathrm{I}}^{(1)} - k_{\mathrm{II}}^{(1)}) + (k_{\mathrm{I}}^{(2)} - k_{\mathrm{II}}^{(2)})]^2 \\ -4(k_{\mathrm{I}}^{(1)} - k_{\mathrm{II}}^{(1)})(k_{\mathrm{I}}^{(2)} - k_{\mathrm{II}}^{(2)})\sin^2 \zeta^{(12)}\end{array}} \quad (14)$$

$$B = \tfrac{1}{4}(k_{\mathrm{I}}^{(1)} + k_{\mathrm{II}}^{(1)} + k_{\mathrm{I}}^{(2)} + k_{\mathrm{II}}^{(2)})$$

$$+ \tfrac{1}{4}\sqrt{\begin{array}{c}[(k_{\mathrm{I}}^{(1)} - k_{\mathrm{II}}^{(1)}) + (k_{\mathrm{I}}^{(2)} - k_{\mathrm{II}}^{(2)})]^2 \\ -4(k_{\mathrm{I}}^{(1)} - k_{\mathrm{II}}^{(1)})(k_{\mathrm{I}}^{(2)} - k_{\mathrm{II}}^{(2)})\sin^2 \zeta^{(12)}\end{array}} \quad (15)$$

where $k_{\mathrm{I}}^{(i)}$ and $k_{\mathrm{II}}^{(i)}$ ($i = 1, 2$) are the principal curvatures of the contact surfaces, and $\zeta^{(12)}$ is the angle formed by the unit vectors of the principal directions. Since the equations of the worm gear drive are known, the principal curvatures of the tooth surfaces can be obtained [13].

4.3 Determination of the distribution of contact pressure

With equation (9), the pressure at the centre of the contact ellipse is determined when the semi-axes are known. Then, the pressure at any position inside the contact ellipse can be obtained using equation (7). To simplify the FE calculation process, the contact ellipse is divided into a number of elements and the pressure on each element of the contact ellipse is assumed as an average pressure, as shown in Fig. 5.

The average pressure can be calculated as

$$\bar{p}_{i,j} = \frac{1}{A_e} \int_{y_{j-1}}^{y_j} \int_{x_{i-1}}^{x_i} p_0 \sqrt{1 - \frac{x^2}{a^2} - \frac{y^2}{b^2}} \, \mathrm{d}x \, \mathrm{d}y \quad (16)$$

where the subscripts i and j represent the position of an element of the contact ellipse, and A_e is the area of the element. Undoubtedly, the more elements the contact ellipse is divided into, the more accurate the calculation result will be.

5 CALCULATION OF THE MESH STIFFNESS OF ENGAGING TOOTH PAIRS

A key factor in determination of the load share among the simultaneously engaged tooth pairs is the mesh stiffness, which is defined as the combined stiffness at the contact position of the engaged tooth pairs. After the tooth modification, the worm gear drive has localized tooth contact, i.e. 'point' or zone contact, and the original meshing principle is not applicable any more. The tooth contact analysis (TCA) method is applied to predict the tooth contact path for the modified worm gear drives and the computation results of TCA represent the theoretical contact positions of the tooth surfaces.

For the case where a pair of teeth is engaged at the contact position, the following assumptions are introduced to simplify the calculation:

1. Tooth deformation is elastic.
2. The centre of the contact ellipses will not shift after the elastic deformation.

During the tooth engaging process, both the worm tooth and the wheel tooth have a deformation under the load, as shown in Fig. 6. The driving force is transmitted at the contact point that is the theoretical contact position of the tooth pair. The sum of elastic deformation includes the deformations of the worm tooth U_1 and the wheel tooth U_2, i.e. $U = U_1 + U_2$.

With respect to an individual tooth, its elastic deformation is composed of two components: bending deformation and contact deformation. The tooth bending compliance is defined as the displacement along the normal to the tooth profile where a unit load is applied, while the tooth contact compliance is defined on the basis of Hertzian assumptions [14]. Because the contact position always shifts during the engagement,
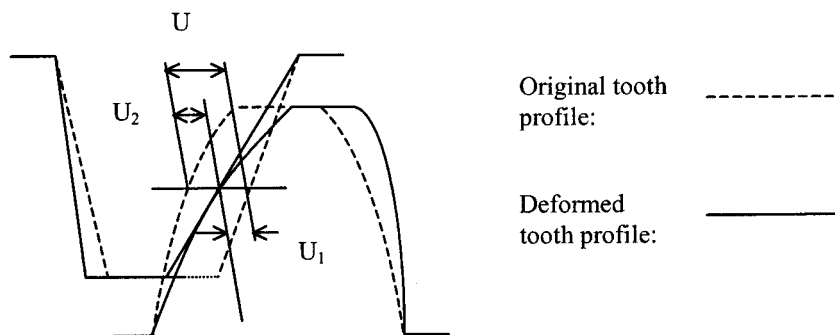
Fig. 6 Tooth deformation under load

the bending and contact compliances, and hence the meshing stiffness, vary over the engaging process.

According to the above assumptions, the magnitude of the deformation $U_i(\delta)$ at the centre of the contact ellipses for the worm U_1 or the wheel U_2 can be recognized as the instantaneous nominal deformation at the meshing position. Applying a load on the FE models of the worm and wheel, the deformation magnitude $U_i(\delta)$ at the centre of the contact ellipse, which includes both bending and contact deformation, can be calculated. Therefore, the instantaneous stiffness for an individual tooth is defined as

$$K_i(\delta) = \frac{F_\delta}{U_i(\delta)} \qquad (17)$$

The instantaneous meshing stiffness at the contact point of the engaging tooth pairs is then

$$K_\delta = \frac{K_1(\delta)K_2(\delta)}{K_1(\delta) + K_2(\delta)} \qquad (18)$$

The contact point moves on the tooth surface during the engaging process and therefore the instantaneous meshing stiffness depends on the contact path of the worm gear drive. Because of different manufacturing errors, the contact path of the worm gear drive changes accordingly. The change affects the meshing stiffness significantly. The meshing stiffness for a worm gear drive is actually a function of contact position which is defined as the meshing stiffness function along the contact path (MSFACP) in this research. The computation of MSFACP is based on the FE models. The load has been assigned to the worm model and the wheel model at respective contact points with Hertzian distribution. The deformation of the contact point is cal-

culated and the stiffness of both worm and wheel are obtained. Figure 7 shows the meshing stiffness of an involute worm gear drive.

6 LOAD SHARE ANALYSIS OF THE WORM GEAR DRIVES

The condition of tooth deformation compatibility determines the load distribution between tooth pairs in contact [15–17]. In gear engagement, two factors may significantly affect the gear transmission. One is the tooth profile error caused by manufacturing and assembly errors and the other is the tooth elastic deformation for both the worm and the wheel, determined by the load acting on the contacting teeth. If the total displacement of the ith tooth pair in contact is represented as Δ_i (Fig. 8), the corresponding rotation increment is then written as Δ_i/R_i, i.e. the extra rotation caused by the total displacement. Therefore, to ensure continuous transmission, it is necessary that every tooth pair in contact has the same rotation increment under load. It can be written as

$$\Delta_{i-1}/R_{i-1} = \Delta_i/R_i = \Delta_{i+1}/R_{i+1} \qquad (19)$$

The total displacement comprises the elastic deformation and the geometric mismatch of the tooth surfaces that is caused by manufacturing and assembly errors. Equation (19) is widely recognized as the compatible condition for tooth deformation [7, 8].

Usually, a worm gear has more than one pair of teeth engaged during the meshing process, and the number of simultaneous contact teeth and the load-sharing percentage among the teeth always vary in the process. The
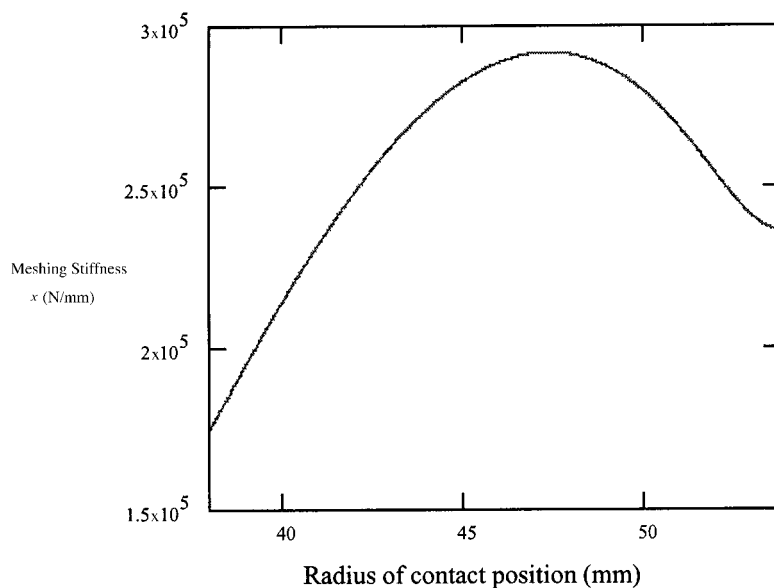

Fig. 7 Meshing stiffness of an involute worm gear drive

contacting tooth pairs have different displacements under load. According to the compatibility condition for smooth tooth rotation, the following conditions must be met in order to maintain smooth motion transmission:

1. The extra tooth rotation angle caused by the displacement under load must be the same for all the simultaneously engaged tooth pairs. Otherwise, continuous smooth transmission is not possible.
2. The sum of the torque contributions of each engaged tooth pair must be equal to the total applied torque.

If there are n tooth pairs in contact simultaneously (Fig. 8), the vectors to describe the total displacement and the rotation increment at each contact point can be expressed as Δ and $\Delta\boldsymbol{\theta}$ respectively:

$$\Delta = \begin{bmatrix} \Delta_1 \\ \Delta_2 \\ \vdots \\ \Delta_n \end{bmatrix} \tag{20}$$

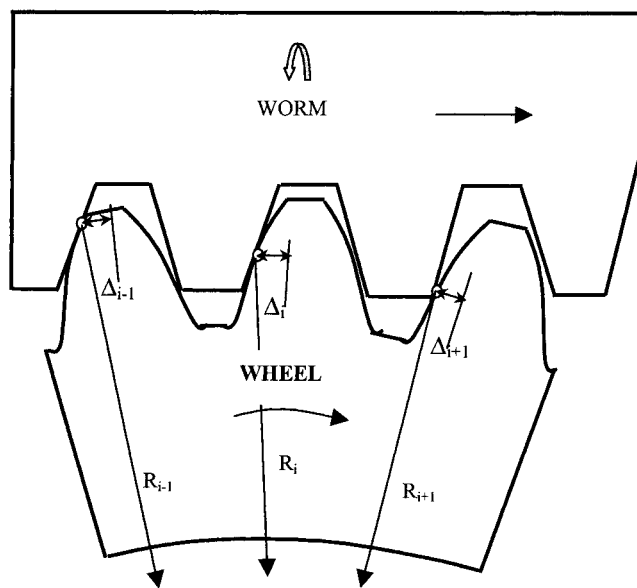$$\Delta\boldsymbol{\theta} = \begin{bmatrix} \Delta\theta_1 \\ \Delta\theta_2 \\ \vdots \\ \Delta\theta_n \end{bmatrix} \tag{21}$$

where $\Delta_1, \Delta_2, \ldots, \Delta_n$ and $\Delta\theta_1, \Delta\theta_2, \ldots, \Delta\theta_n$ refer to the displacement and rotation increment at the contact point of each meshing tooth pair. The radius matrix for the worm gear drives is written as

$$[\mathbf{R}] = \begin{bmatrix} R_1 & & & 0 \\ & R_2 & & \\ & & \cdots & \\ 0 & & & R_n \end{bmatrix} \tag{22}$$

where $R_1, R_2, \ldots, R_n$ represent the radius of each contact point of the respective tooth pair. The vector for torque distribution is written as

$$\boldsymbol{d} = \begin{bmatrix} d_1 \\ d_2 \\ \vdots \\ d_n \end{bmatrix} \tag{23}$$

where $d_1, d_2, \ldots, d_n$ are the torque share coefficients of the respective contact tooth pair. Therefore, the load vector is expressed as

$$\boldsymbol{T} = T \cdot \boldsymbol{d} \tag{24}$$

It is obvious that the sum of the coefficients is equal to one, and therefore

$$\sum_{i=1}^{n} d_i = 1 \tag{25}$$

The contact force at the theoretical contact position is defined as

$$\boldsymbol{P} = [\mathbf{R}]^{-1} \cdot \boldsymbol{T} = T \cdot [\mathbf{R}]^{-1} \cdot \boldsymbol{d} \tag{26}$$

For each pair of contact teeth, there are bending elastic deformation and contact elastic deformation in the contact area. It is assumed that the load is applied at the contact point and the contact is spread over an elliptical area whose centre remains the theoretical contact point. The vector to depict the elastic deformation is written as

$$\boldsymbol{\delta} = \begin{bmatrix} \delta_1 \\ \delta_2 \\ \vdots \\ \delta_n \end{bmatrix} \tag{27}$$

where $\delta_1, \delta_2, \ldots, \delta_n$ refer to the elastic deformations at each contact point of the respective tooth pair. The

Fig. 8 Condition of deformation compatibility

matrix of meshing stiffness represents the local meshing stiffness at each contact point. It is written as

$$[\mathbf{K}] = \begin{bmatrix} K_{\delta 11} & & & 0 \\ & K_{\delta 22} & & \\ & & \cdots & \\ 0 & & & K_{\delta nn} \end{bmatrix} \qquad (28)$$

Therefore, the sum of elastic deformation can be represented as

$$P = T \cdot [\mathbf{R}]^{-1} \cdot d = [\mathbf{K}] \cdot \delta$$
$$\delta = T \cdot [\mathbf{K}]^{-1} \cdot [\mathbf{R}]^{-1} \cdot d \qquad (29)$$

According to the motion relation of worm gear drives, the relation between the displacement increment and rotation increment can be written as

$$\boldsymbol{\Delta} = [\mathbf{R}] \cdot \Delta \boldsymbol{\theta} \qquad (30)$$

The transmission error at the contact point of every simultaneously meshing tooth pair can be represented as

$$\Delta \boldsymbol{\varphi} = \begin{bmatrix} \Delta \varphi_1 \\ \Delta \varphi_2 \\ \vdots \\ \Delta \varphi_n \end{bmatrix} \qquad (31)$$

Therefore, the displacement caused by the transmission error is written as

$$\boldsymbol{\tau} = [\mathbf{R}] \cdot \Delta \boldsymbol{\varphi} \qquad (32)$$

The total displacement of the contact tooth pairs under load can be described as the sum of elastic deformation (both bending and contact deformation) and transmission error (the tooth profile separation caused by manufacturing error or misalignment):

$$\boldsymbol{\Delta} = \boldsymbol{\delta} + \boldsymbol{\tau} \qquad (33)$$

Introducing equations (29), (30) and (32) into equation (33) gives

$$[\mathbf{R}] \cdot \Delta \boldsymbol{\theta} = T \cdot [\mathbf{K}]^{-1} \cdot [\mathbf{R}]^{-1} \cdot d + [\mathbf{R}] \cdot \Delta \boldsymbol{\varphi} \qquad (34)$$

From the condition of deformation compatibility, to ensure continuous transmission, it is necessary that every tooth pair in contact has the same rotation increment under load, e.g.

$$\Delta \theta_1 = \Delta \theta_2 = \cdots = \Delta \theta_n = \Delta \theta$$

Therefore, $\Delta \boldsymbol{\theta}$ can be expressed as

$$\Delta \boldsymbol{\theta} = \Delta \theta \begin{bmatrix} 1 \\ 1 \\ \vdots \\ 1 \end{bmatrix} = \Delta \theta [1] \qquad (35)$$

Therefore, equation (23) can be transformed into

$$d = \frac{1}{T} \cdot [\mathbf{R}] \cdot [\mathbf{K}] \{ [\mathbf{R}] \cdot \Delta \theta - [\mathbf{R}] \cdot \Delta \varphi \}$$
$$= \frac{1}{T} [\mathbf{R}] \cdot [\mathbf{K}] \cdot [\mathbf{R}] \cdot \{ \Delta \theta - \Delta \varphi \} \qquad (36)$$

and $\Delta \theta$ can be determined as follows:

$$\sum_{i=1}^{n} d_i = 1$$

Therefore

$$\sum_{i=1}^{n} \left(\frac{1}{T} [\mathbf{R}] \cdot [\mathbf{K}] \cdot [\mathbf{R}] \cdot \{ \Delta \theta - \Delta \varphi \} \right) = 1 \qquad (37)$$

and

$$\Delta \theta = \frac{T + \sum_{i=1}^{n} [\mathbf{R}] \cdot [\mathbf{K}] \cdot [\mathbf{R}] \cdot \Delta \varphi}{\sum_{i=1}^{n} [\mathbf{R}] \cdot [\mathbf{K}] \cdot [\mathbf{R}] \cdot [1]} \qquad (38)$$

If no transmission error exists, e.g. $\Delta \varphi = 0$, then

$$\Delta \theta = \frac{T}{\sum_{i=1}^{n} [\mathbf{R}] \cdot [\mathbf{K}] \cdot [\mathbf{R}] \cdot [1]} \qquad (39)$$

where T is the total torque and θ is the nominal increment in the rotation angle, which is determined by material, tooth geometry, load and errors caused by misalignment. Then, d can be calculated using equation (36), and therefore the load distribution is obtained.

Figure 9 shows the complete load share description for a pair of teeth in the process of engagement from the moment of starting contact until finishing contact. Observing the above, the following can be derived regarding the load share of the tooth pairs:

1. At the starting contact position, where the tip of the wheel tooth and the root of the worm tooth are in contact, the load share of the engaged tooth pair is quite small. Because of the low stiffness of the wheel tooth tip, the meshing stiffness of the starting position is lower as well. Therefore, the tooth pair only shares a low percentage of the load.

2. At the final contact position, where the root of the wheel tooth and the tip of the worm tooth are in
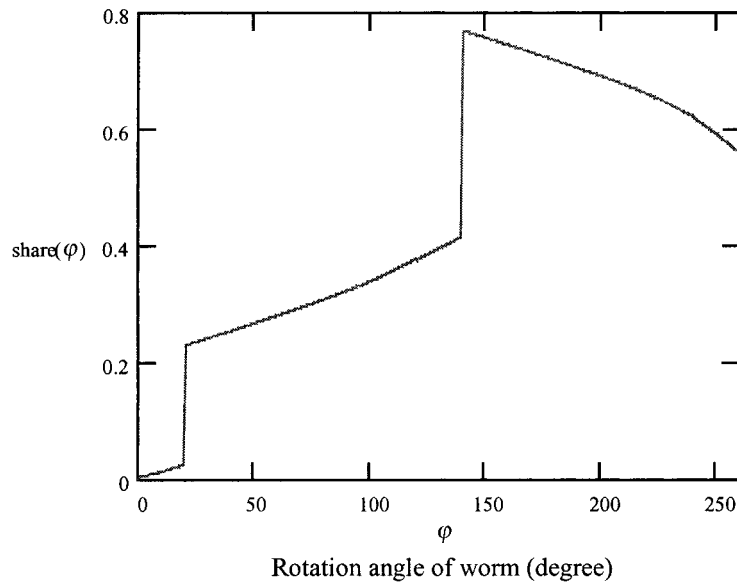
Fig. 9 Load share by a pair of teeth on a worm gear drive

contact, the load share of the engaged tooth pair remains at about 50 per cent of the load. This means that the tooth pair of the worm gear still bears a high load before quitting the engagement. Because the worm tooth tip and the wheel tooth root both have a higher stiffness, the meshing stiffness of the final position is much higher than that of the starting position. Hence, the tooth pair shares a higher percentage of the load.

3. When the worm rotation angle is about 140°, the tooth pair bears the highest percentage of the load (76.9 per cent).

4. When the other tooth pair is getting into or out of the engagement, there are abrupt changes in the load share of the tooth pair at that moment. The abrupt change is the main cause of impact vibration in worm gear drives.

7 DETERMINATION OF THE TRANSMISSION ERRORS UNDER LOAD

The real transmission error under load is determined by the actual total displacement of the contact tooth pairs, which is affected by the elastic deflection of the loaded tooth body. The total displacement can be represented as the sum of the elastic deformation and the theoretical transmission error (the tooth profile separation caused by manufacturing error or misalignment) as shown below:

$$\Delta = \delta + \tau \tag{40}$$

where δ is the vector depicting the elastic deformation and τ is the vector depicting the displacement caused by

theoretical transmission errors. Since the elastic deformation at every instant of the engagement can be determined using FE analysis with the real load share of the tooth pair, the total displacement at the contact position is written as $\Delta_i = \delta_i + \tau_i$.

The real transmission error under load can be described as

$$\mathrm{TE}_i = \frac{\Delta_i}{R_i} = \frac{\delta_i}{R_i} + \frac{\tau_i}{R_i} = \frac{\delta_i}{R_i} + \Delta\varphi_i \tag{41}$$

where R_i is the radius of the contact position and $\Delta\varphi_i$ is the theoretical transmission error without considering the load. Because the theoretical transmission error τ_i has been obtained from TCA, the transmission error under load can be determined. It is obvious that under load the transmission error is different from the theoretical one.

A calculation procedure has been developed to determine the transmission error under load. The procedure includes the TCA process, the meshing stiffness calculation using the FE model and load share determination for the engaging tooth. The real transmission error of a worm gear drive has been evaluated under different assembly errors and loads. According to the calculation results, under the normal load the tooth elastic deformation of the worm gear is comparable with the displacement caused by the theoretical transmission error (tooth gap caused by the manufacturing error). Therefore, the real transmission error of worm gear drives is a load-dependent function. The approach developed here enables evaluation of the real transmission error under load, which is especially valuable for high-speed transmissions.

The loaded transmission errors of the worm gear drive under different loads are shown in Fig. 10. It can
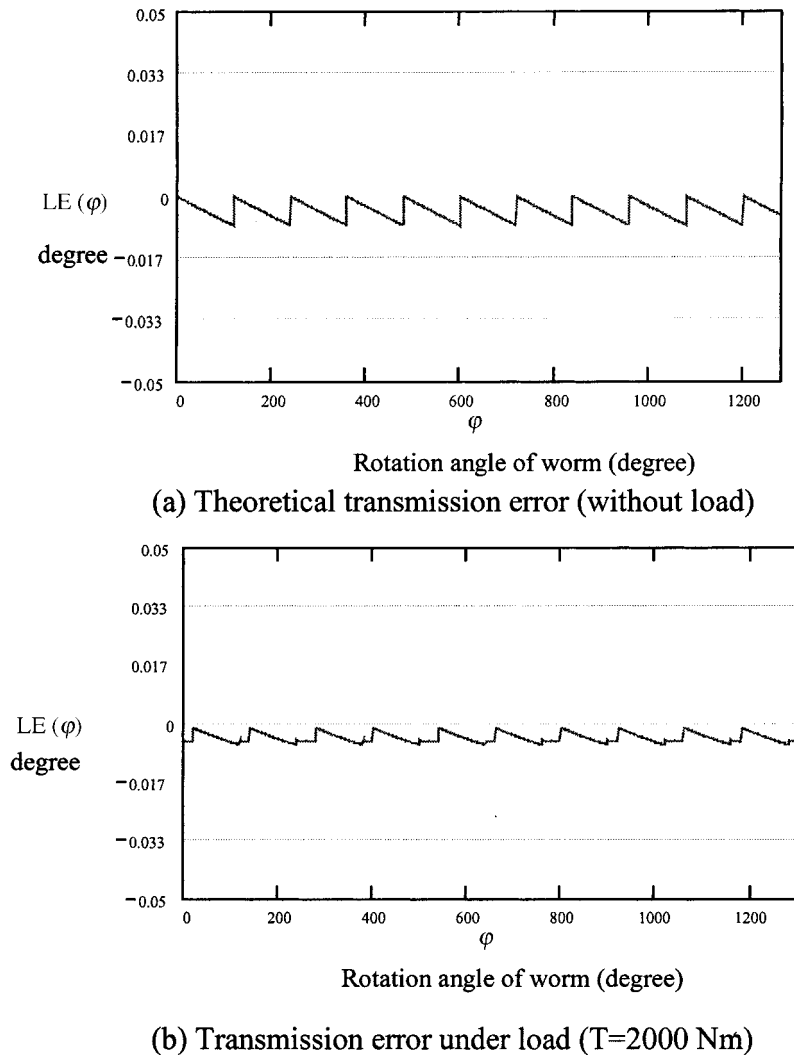
(a) Theoretical transmission error (without load)

(b) Transmission error under load (T=2000 Nm)

Fig. 10 Transmission errors of the worm gear drive

be seen that under certain load the transmission error has been significantly reduced. This can be interpreted as showing that the elastic deformation under load can compensate for the tooth gap caused by the manufacturing error. Following the above conclusion, it is clear that the transmission error will change substantially under load.

8 CONCLUSIONS

In this paper, a method of FE modelling and load share analysis for worm gear drives with localized tooth contact has been developed. The elastic three-dimensional FE models of the worm and wheel are created using ANSYS software, and appropriate elements are chosen to mesh the model.

The FE analysis is applied for the worm gear drive with modified tooth geometry. From the results of the FE analysis, the instantaneous meshing stiffness and transmission error under load are obtained and the load share of the worm gear drives is estimated. The results are important for rating the load capacity and very useful in the design of worm gear drives with compact size and high loading capacity.

Although this study is aimed at involute worm gears, the proposed method is quite general and can be applied to predict the deformation, stress and loaded transmission error for other gears.

REFERENCES

1 **Janninck, W. L.** Contact surface topology of worm gear teeth. *Gear Technol.*, 1988, **5**(2), 31–47.
2 **Colbourne, J. R.** The use of oversized hobs to cut wormgears. AGMA technical paper 89FTM8, 1989 (American Gear Manufacturers Association, Alexandria, Virginia).
3 **Vinula, H., Miloiu, G., Visa, F.** and **Tiscanu, C.** Numerical

research regarding contact localisation at cylindrical worm gears. In Proceedings of 9th World Congress on *Theory of Machine and Mechanisms*, Milan, 1995, pp. 442–446.

4 Yoshino, H. and **Muta, Y.** Tooth surface modification method applicable to various types of worm gears. In Proceedings of International Conference on *Mechanical Transmissions and Mechanisms*, Tianjin, China, 1–4 July 1997, pp. 598–602.

5 Seol, I. H. and **Litvin, F. L.** Computerised design, generation and simulation of meshing and contact of modified involute, Klingelnberg and Flender type worm-gear drives. *Trans. ASME, J. Mech. Des.*, 1996, **118**, 551–555.

6 Litvin, F. L. and **Kin, V.** Computerised simulation of meshing and bearing contact for single enveloped worm-gear drives. *Trans. ASME, J. Mech. Des.*, 1992, **114**, 313–316.

7 Litvin, F. L., Chen, J. S., Lu, J. and **Handschuh, R. F.** Application of finite element analysis for determination of load share, real contact ratio, precision of motion, and stress analysis. *J. Mech. Des.*, 1996, **118**(4), 561–567.

8 Gosselin, C., Cloutier, L. and **Nguyen, Q. D.** A general formulation for the calculation of the load sharing and transmission error under load of spiral bevel and hypoid gears. *Mechanism and Mach. Theory*, 1995, **30**(3), 433–450.

9 Yang, F., Wang, X., Su, D. and **Gentle, C. R.** A numerical method to obtain preferable localised tooth contact for cylindrical worm gearing. In Proceedings of International Conference on *Mechanics in Design*, Nottingham, UK, 6–9 July 1998, pp. 149–157.

10 Su, D., Yang, F., Gentle, C. R. and **Reith, D.** A new approach combining numerical analysis and three-dimensional simulation for design of worm gearing with preferable localised tooth contact. In Proceedings of 25th ASME Biennial Mechanisms Conference, Georgia, USA, 13–16 September 1998, paper DETC98/MECH-5830.

11 *ANSYS User's Manual for Version 5.3*, 1994, Vol. 1 (Swanson Analysis Systems, Houston, Pennsylvania).

12 Boresi, A. P. and **Sidebottom, O. M.** *Advanced Mechanics of Materials*, 1985 (John Wiley, Chichester).

13 Yang, F. Numerical analysis and 3D modelling and simulation of worm gearing with localised tooth contact. PhD dissertation, The Nottingham Trent University, Nottingham, UK.

14 Zhang, J. J., Esat, I. I. and **Shi, Y. H.** Load analysis with varying mesh stiffness. *Computers and Struct.*, 1999, **70**(3), 273–280.

15 Lu, J., Litvin, F. L. and **Chen, J. S.** Load share and finite element stress analysis for double circular-arc helical gears. *Math. and Computer Modelling*, 1995, **21**(10), 13–30.

16 Sudoh, K., Tanaka, Y., Matsumoto, S. and **Tozaki, Y.** Load distribution analysis method for cylindrical worm gear teeth. *Jap. Soc. Mech. Engrs Int. Ser. C, Dynamics Control Robotics Des. and Mfg*, 1996, **39**(3), 606–613.

17 Simon, V. Load distribution in double enveloping worm gears. *Trans. ASME, J. Mech. Des.*, 1993, **115**, 496–500.